2nd Symposium on New Trends in Nuclear and Medical Physics, Poland, September 24–26, 2025

Developing Analysis Criteria for Charge–Parity Symmetry Studies Using Photons From Ortho-Positronium Annihilation and Compton Scattering

K.V. Eliyan[a,b,*], M. Skurzok[a,b] and P. Moskal[a,b]
(on Behalf of the J-PET Collaboration)

[a] *Faculty of Physics, Astronomy and Applied Computer Science, Jagiellonian University, Łojasiewicza 11, 30-348 Kraków, Poland*
[b] *Center for Theranostics, Kopernika Street 40, 31-501 Kraków, Poland*

Doi: 10.12693/APhysPolA.148.S115 *e-mail: kavya.eliyan@doctoral.uj.edu.pl

The main aim of this research is to test the charge–parity discrete symmetry in the ortho-positronium (o-Ps) atom decay using the modular Jagiellonian positron emission tomography (J-PET) detector. The J-PET is distinguished by its ability to determine the polarization plane of photons emitted during positronium annihilation. The J-PET detector can investigate discrete symmetry by examining the non-zero expectation values of the symmetry-odd operators constructed from the momentum and direction of polarization plane of gamma (γ) quanta coming from o-Ps annihilation. In positronium decay, the photon–photon interactions in the final state due to vacuum polarization may mimic a charge–parity symmetry violation at the level of 10^{-9}, according to the Standard Model prediction. Currently, with the help of the 192-strip J-PET detector, the experimental limits on charge–parity symmetry violation in o-Ps decay are set at a precision value of 0.0005 ± 0.0007. Using the modular J-PET detector, we aim to improve this value by at least an order of magnitude. This article focuses on developing analysis criteria towards improving the sensitivity level for charge–parity-discrete symmetry studies in o-Ps decay using the modular J-PET detector.

topics: positronium, polarization, charge–parity (CP) symmetry, Jagiellonian positron emission tomography (J-PET)

1. Introduction

A novel approach is being developed using the Jagiellonian positron emission tomography (J-PET) detector to test discrete symmetries in ortho-positronium (o-Ps) decays using the polarization of annihilation photons [1–8]. The angular correlation operator ($\boldsymbol{\epsilon}_i \cdot \boldsymbol{k}_j$) — which is odd under the charge–parity (CP), parity (P), and time-reversal (T) transformations — has been used, hence making possible to test CP symmetry in positronium decays [1–12]. The CP symmetry is investigated by determining the expectation value of the operator calculated as a mean of the $\cos(\theta_{ij})$ spectrum, defined as

$$\cos(\theta_{ij}) = \frac{\boldsymbol{\epsilon}_i \cdot \boldsymbol{k}_j}{|\boldsymbol{\epsilon}_i|\,|\boldsymbol{k}_j|}, \tag{1}$$

where θ_{ij} is the angle between $\boldsymbol{\epsilon}_i$ and $\boldsymbol{k}_j$ [1–7]. The vector $\boldsymbol{\epsilon}_i$ is constructed as the cross product of the momentum vector direction of one annihilation photon before ($\boldsymbol{k}_i$) and after Compton scattering ($\boldsymbol{k}_i{}'$) in the detector, i.e., $\boldsymbol{\epsilon}_i = \boldsymbol{k}_i \times \boldsymbol{k}_i{}'$. The momentum vector direction of another annihilation photon in the same o$-$Ps $\rightarrow 3\gamma$ decay event, — other than a photon with momentum vector ($\boldsymbol{k}_i$) — is represented as $\boldsymbol{k}_j$ [1, 4–8]. The non-zero expectation value of the operator refers to a violation of the studied symmetry. Recently published J-PET studies performed, based on data collected with the 192-strip J-PET detection system, gave a mean expectation value of 0.0005 ± 0.0007 for this operator [4]. The goal of using the modular J-PET detector is to attain a 5-fold improved precision level in the expectation value of the CP odd operator [4–8].

2. Measurements and analysis

The modular J-PET detector is a newly developed, flexible, and portable variant of the J-PET detection system [13–21]. Measurements for the CP symmetry study were carried out using the modular J-PET detector that has 20 times higher sensitivity for o$-$Ps $\rightarrow 3\gamma$ signal registration compared to the 3-layer prototype detector [21–27]. The arrangement of plastic scintillators in the modular J-PET detector is shown in Fig. 1a [13–18, 24, 26].

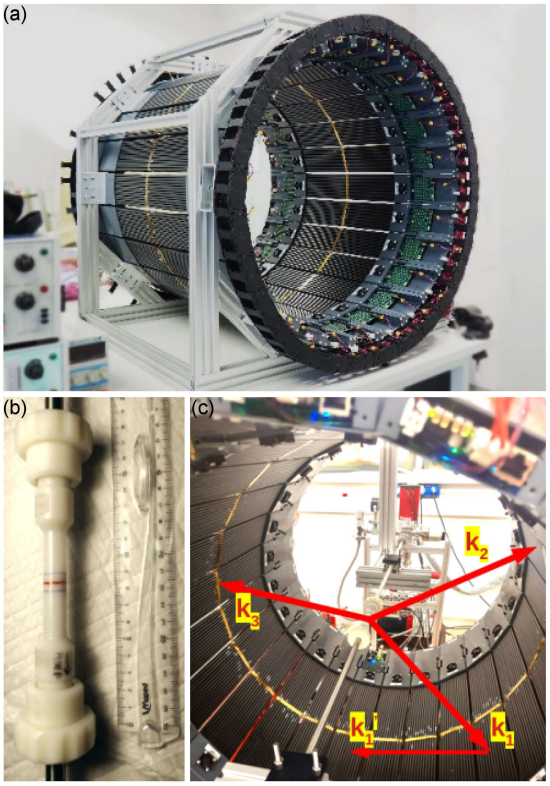

Fig. 1. (a) Modular J-PET detector [13–18,24,26]. (b) ^{22}Na point source embedded in XAD-4 porous polymer placed at the center (red line) of the small annihilation chamber. (c) The small annihilation chamber is placed at the center of the modular setup, and the schematic (red) shows o–Ps $\rightarrow 3\gamma$+1 Compton-scattered signal event [4–8].

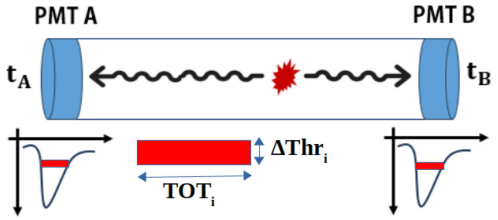

Fig. 2. Red dot indicates a photon hit in the scintillator strip, and signals are read by two photomultipliers (PMT A and PMT B) placed at two sides of the scintillator strip [1–8].

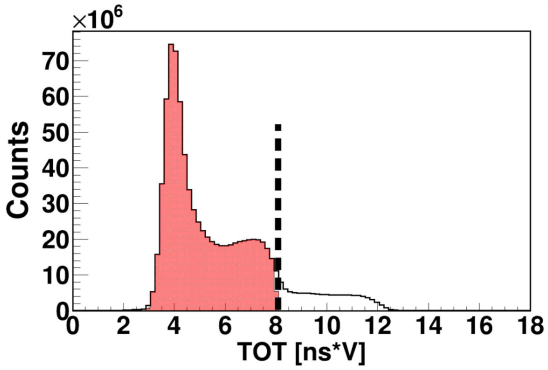

Fig. 3. Experimental TOT spectrum for all hits (black line). The black dashed line at $8 n_s\, V$ indicates the Compton edge for annihilation photons. Hits with TOT values between $3 \leq$ TOT ≤ 8 ns V are selected as annihilation candidates (red region).

A small annihilation chamber (PA6 material) containing a sodium source with an activity of 5.541 MBq was placed at the center of the detector (Fig. 1b and c). The superimposed arrows (red) in Fig. 1c indicate the momentum vector directions of the primary photons from the o-Ps decay ($\boldsymbol{k}_1, \boldsymbol{k}_2, \boldsymbol{k}_3$) and the secondary Compton-scattered photon ($\boldsymbol{k}_i{}'$). Using this modular experimental setup, a total of 138 days of measurement was performed. As a part of developing analysis criteria for the CP symmetry study, we present here the results from a preliminary analysis of one hour of the modular experimental data. In the coming month, Monte Carlo simulation studies will be conducted for the optimization of signal selection criteria, and after that, we will perform a full experimental data analysis.

Analysis of the experimental data was performed using the J-PET Analysis Framework software, which consists of several modules [1–8]. Each of them corresponds to a particular computing task, such as calibration procedure and reconstruction algorithm [1–8]. This analysis requires hits in the scintillators, which are grouped into clusters within a defined time window (200 ns). Such grouped hits are referred to as 'events'. For this study, the signal hits of interest originate from o-Ps $\rightarrow 3\gamma$ accompanied with one Compton-scattered photon [1–8]. In order to minimize contributions from the photons scattering in the detector housing, signals from the edges of the scintillators were excluded. So, as the first analysis step, hits are chosen only if their reconstructed Z coordinate falls between -23.0 cm and $+23.0$ cm along the scintillator strips. This restriction decreases the chances of getting background hits from the region outside the active scintillator area [1–8]. When the condition $|Z| \leq 23$ cm is met, events with a hit multiplicity ≥ 4 are selected. For each hit read by the photomultiplier tube (PMT), the time-over-threshold (TOT) value is calculated by the rectangular method on all available thresholds (30 mV and 70 mV) applied to PMT (Fig. 2). The TOT parameter is considered as the measure of energy deposited by a photon once it hits on the scintillator strip [1–8]. The TOT values for the signal read by the PMT and from the photon hit are given, respectively, by

$$\mathrm{TOT}_{\mathrm{signal}} = \sum_{i=1}^{2} \mathrm{TOT}_i \, \Delta\mathrm{Thr}_i, \tag{2}$$

$$\mathrm{TOT}_{\mathrm{hit}} = \mathrm{TOT}^{\mathrm{A}}_{\mathrm{signal}} + \mathrm{TOT}^{\mathrm{B}}_{\mathrm{signal}}, \tag{3}$$

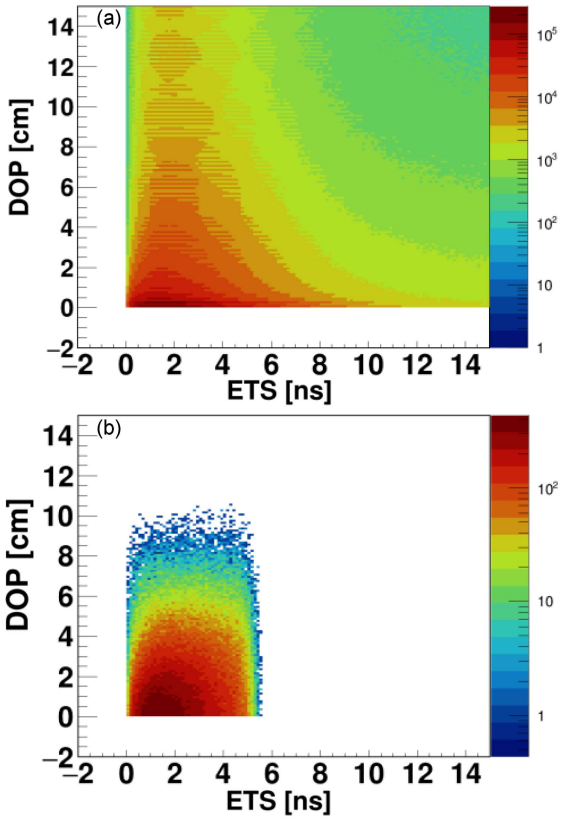

Fig. 4. ETS vs DOP plot before (a) and after (b) selecting the best triplet hit that gives the smallest R value in an event.

where $\Delta\mathrm{Thr}_i = \mathrm{Thr}_i - \mathrm{Thr}_{i-1}$ and $\mathrm{Thr}_0 = 0$. Both TOT_i and $\Delta\mathrm{Thr}_i$ are shown in Fig. 2. The parameter TOT_i is the difference between the trailing time and the leading time of the signal at threshold i.

Figure 3 shows the experimental TOT spectrum, with the red shadowed area corresponding to the time-over-threshold of the annihilation photon and the secondary hits of the scattered photons. Throughout the analysis, the annihilation point is assumed to be at the center of the detector, and the annihilation photons are expected to lie in a single plane [4–8]. The distance of annihilation plane (DOP) is the distance between the annihilation point and the reconstructed plane formed by the three detected hits [1–8]. Also, for each triplet, the difference between the emission times of the third and first hit in an event is calculated, which is defined as the emission time spread (ETS) [1–8], where the emission time is the difference between the photon travel time and the registered hit time [1–8]. For each event, all possible triplet hit combinations are considered, and the ETS vs DOP plot is shown in Fig. 4a. The best triplet hits are chosen by minimizing the parameter R given by [4–8]

$$R = \sqrt{\left(\frac{\mathrm{DOP}}{\sigma_{\mathrm{DOP}}}\right)^2 + \left(\frac{\mathrm{ETS}}{\sigma_{\mathrm{ETS}}}\right)^2}. \qquad (4)$$

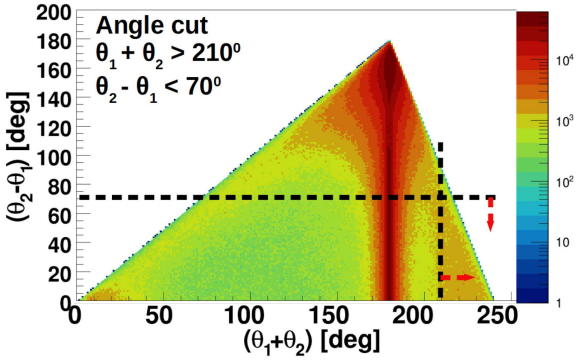

Fig. 5. Sum of the two smallest relative angles $(\theta_1 + \theta_2)$ versus their difference $(\theta_2 - \theta_1)$ plot. o-Ps candidates are visible in the region marked by dashed lines with pointing arrows ($\theta_1 + \theta_2 > 210^\circ$ and $\theta_2 - \theta_1 < 70^\circ$).

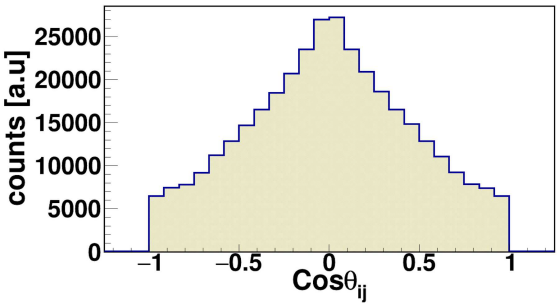

Fig. 6. Preliminary $\cos(\theta_{ij})$ plot obtained at a precision level of 0.0002 ± 0.0007 from one hour of modular experimental data analyzed.

Those selected triplet hits for which the value of R is closest to zero are true candidates for the photon hits from o-Ps $\rightarrow 3\gamma$ decay (Fig. 4b).

The relative angles between the hits in the best triplet chosen are calculated; they are ordered from the smallest to the largest [1–8]. In the 2D relative angle plot (Fig. 5), the events corresponding to o-Ps $\rightarrow 3\gamma$ decay are clearly visible in the regions $(\theta_1 + \theta_2) > 210^\circ$ and $(\theta_2 - \theta_1) < 70^\circ$ [1–8]. To assign a secondary scattered hit to a primary annihilation hit, a scatter test was performed between each pair of hits, and the hit pair that gives the smallest scatter test value (STV) was chosen [4–8].

After applying all the signal selection criteria, three independent CP odd operators $(\boldsymbol{\epsilon}_1 \cdot \boldsymbol{k}_2)$, $(\boldsymbol{\epsilon}_2 \cdot \boldsymbol{k}_3)$, $(\boldsymbol{\epsilon}_3 \cdot \boldsymbol{k}_1)$ are constructed, and their expectation values are calculated using (1). The $\cos(\theta)$ plot for all the operators is shown in Fig. 6.

3. Conclusions

Using the 192-strip J-PET detector, the statistical precision achieved so far in studies of CP discrete symmetry in o-Ps decay is 0.0005 ± 0.0007 [4].

The preliminary results from one hour experimental data analysis shows a precision level of 0.0002 ± 0.0007 obtained using the modular J-PET detector. The modular J-PET detector [28] is aiming to improve the mean expectation value of the CP-odd operator by an order of magnitude after analysing 100% of the experimental data sample. Monte Carlo simulation studies will be conducted to optimize the signal selection criteria for the construction of the CP symmetry odd operator and to evaluate their expectation value precision.

Acknowledgments

The authors acknowledge support from the National Science Centre of Poland through grants MAESTRO no. 2021/42/A/ST2/00423, OPUS no. 2021/43/B/ST2/02150, OPUS24 + LAP no.2022/47/I/NZ7 /03112 and, SONATA no. 2023/50/E/ST2/00574, the Ministry of Science and Higher Education through grant no. IAL/SP/596235/2023, the SciMat and qLife Priority Research Areas budget under the program Excellence Initiative — Research University at Jagiellonian University. We also acknowledge Polish high-performance computing infrastructure PLGrid (HPC Center: ACK Cyfronet AGH) for providing computer facilities and support within the computational grant no. PLG/2024/017688.

References

[1] P. Moskal, D. Alfs, T. Bednarski et al., *Acta Phys. Pol. B* **47**, 509 (2016).

[2] P. Moskal, D. Kumar, S. Sharma et al., *Sci. Adv.* **11**, 18 (2025).

[3] S. Bass, *Acta Phys. Polon. B* **50**, 1319 (2019).

[4] P. Moskal, E. Czerwiński, J. Raj et al., *Nat. Commun.* **15**, 78 (2024).

[5] P. Moskal, A. Gajos, M. Mohammed et al., *Nat. Commun.* **12**, 5658 (2021).

[6] K.V. Eliyan, M. Skurzok, P. Moskal *Acta Phys. Pol. B* **15**, A10 (2022).

[7] K.V. Eliyan, M. Skurzok, P. Moskal *Acta Phys. Pol. B* **17**, A3 (2024).

[8] P. Moskal, N. Krawczyk, B.C. Hiesmayr et al., *Eur. Phys J. C* **78**, 970 (2018).

[9] W. Bernreuther, U. Löw, J.P. Ma, O. Nachtmann, *Phys. C Part. Fields* **41**, 143 (1988).

[10] B.K. Arbic, S. Hatamian, M. Skalsey, J. Van House, W. Zheng, *Phys. Rev. A* **37**, 3189 (1988).

[11] T. Yamazaki, T. Namba, S. Asai, T. Kobayashi, *Phys. Rev. Lett.* **104**, 083401 (2010).

[12] S.D. Bass, S. Mariazzi, P. Moskal, E. Stępień, *Rev. Mod. Phys.* **95**, 021002 (2023).

[13] S. Niedzwiecki, P. Białas, C. Curceanu et al., *Acta Phys. Pol. B* **48**, 1567 (2017).

[14] P. Moskal, S. Niedźwiecki, T. Bednarski et al., *Nucl. Instrum. Methods Phys. Res. A* **764**, 317 (2014).

[15] P. Moskal, E. Stępień, *PET Clin.* **15**, 439 (2020).

[16] P. Moskal, T. Bednarski S. Niedźwiecki et al., *IEEE Trans. Instrum. Meas.* **70**, 2000810 (2021).

[17] P. Moskal, P. Kowalski, R.Y. Shopa et al., *Phys. Med. Biol.* **66**, 175015 (2021).

[18] A. Porcelli, K.V. Eliyan, G. Moskal et al., *Universe* **11**, 180 (2025).

[19] T. Kaplanoglu, P. Moskal, *Bio-Algorithms Med-Syst.* **19**, 109 (2023).

[20] F. Tayefi Ardebili, P. Moskal, *Bio-Algorithms Med-Syst.* **19**, 132 (2023).

[21] P. Moskal, E.Ł. Stepien, *Bio-Algorithms Med-Syst.* **17**, 311 (2021).

[22] M. Kozani, A. Rucinski, P. Moskal, *Bio-Algorithms Med-Syst.* **19**, 23 (2023).

[23] Ł. Kapłon, G. Moskal, *Bio-Algorithms Med-Syst.* **17**, 191 (2021).

[24] Ł. Kapłon, *IEEE Trans. Nucl. Sci.* **67**, 2286 (2020).

[25] A. Gajos, *Symmetry* **12**, 1268 (2020).

[26] E. Czerwiński, J. Raj, J-PET Collaboration *EPJ Web Conf.* **262**, 01009 (2022).

[27] F. Tayefi Ardebili, P. Moskal, *Bio-Algorithms Med-Syst.* **20**, 9 (2024).

[28] P. Moskal, J. Baran, S. Bass et al., *Sci. Adv.* **10**, 37 (2024).